

Electronic Supplementary Information

Sensitive discrimination of single nucleotide variant using PDA microtube waveguide platform with heterogeneous CHA amplification and competitive inhibition strategy

Funing Liu,^{‡a} Junjie Cheng,^{‡a} Xiaohui Feng,^b Kexin Yang,^a Hongli Zhang,^a Jingang Hu,^a Mengqiao Wang,^a Yue Yu,^{*b} Qijin Zhang,^a Gang Zou^{*a}

^aCAS Key Laboratory of Soft Matter Chemistry, Department of Polymer Science and Engineering, iChEM, University of Science and Technology of China, Hefei, Anhui 230026, P. R. China

^bDivision of Gastroenterology, The First Affiliated Hospital of USTC, Division of Life Science and Medicine, University of Science and Technology of China, Hefei, Anhui 230026, P. R. China

*Correspondence and requests for materials should be addressed to E-mail: gangzou@ustc.edu.cn or yuyuemd@ustc.edu.cn

Reagents and instruments

All oligonucleotides used in this work were purchased from Shanghai Bio-Engineering Company (Shanghai, China), and the sequences of DNA and miRNA used in this work were shown in Table S1. The monomer 10, 12-pentacosadiynoic acid used for PDA was purchased from Tokyo Chemical Industry Co., Ltd., and purified to remove the polymerized part before use. Ethylenediamine-substituted Pentacosadiacetylene (EPDA) were synthesized in analogy to the previous procedure.¹ All other solvents and reagents were of analytical grade and used as received. Milli-Q water (18.2 MΩ · cm) was used in all cases. Human serum samples were collected from Anhui Provincial Hospital. Oligonucleotides were quantified by UV-vis absorption spectroscopy, using a SHIMADZU UV-2550 PC spectrophotometer. Fluorescence spectra were measured by a JY-ihR 550 spectrophotometer. Optical microscopy images were obtained in a BX-51 fluorescence microscope. The Raman characterization was performed with a LABRAM-HR Confocal Laser Micro Raman Spectrometer with 514.5 nm radiation at room temperature.

PDA microtubes were prepared using a similar procedure described in the literature.¹ Amine-functionalized PDA microtubes were prepared by a hierarchical self-assembly method.² Then aqueous solution of glycol diglycidyl ether (200 μL, 3 mmol) was added dropwise to PDA microtubes to form epoxy-functionalized PDA microtubes since one of the epoxy group in the glycol diglycidyl ether has great tendency to react with amino group on the surface of PDA microtubes.³ Then DNA Probe-1 (5'-NH-CTATAGGCGAACGATTAACCTAC-3') modified PDA microtubes were prepared as described in Fig. S1. Finally, BHQ3@PDA composite microtubes were prepared through DNA hybridization process between Probe-1 and Probe-2 (5'-AATCGTTCGCCTATAG-BHQ3-3'). The preparation process was monitored by Raman spectroscopic analysis (as shown in Fig. S2).

Probe design principle and Analytic framework

In the present work, we proposed a system integrated two subsystems for the discrimination of SNV at low concentration, one is a subsystem composed of catalytic hairpin assembly (CHA) working as an amplification circuit, and the other is a competitive inhibition system to reduce the signal produced from SNV. To distinguish let-7a, let-7c, let-7e and let-7f simultaneously, a series of amplification and competitive probes were designed as listed in Table S1. In the proposed CHA amplification process, one target (T) can catalyze two hairpin probes (H1, H2) to form a duplex and yield multiple signal outputs. H' used in competitive inhibition process is aimed to bind with the

mutant target that containing specific SNV and suppress its signal. We could increase the sensitivity and decrease the background simultaneously, the possible reason are two-fold. First, unlike traditional CHA in solution, we proposed a novel heterogeneous CHA (hetero-CHA) design integrating with PDA microtube waveguide system, offering the advantages to enhance the target signal, but suppress the background leakage simultaneously.⁴ In heterogeneous CHA amplification strategy, single-stranded (ss-) target miRNA can be enriched onto the surface of PDA microtube due to strong attraction (cation- π interactions between the nucleobase in ss-miRNA and amine cation on the surface of PDA microtube), facilitating the target triggered CHA circuit and strand displacement reactions on the surface of PDA microtube. While the double-stranded (ds-) DNA duplex generated by the uncatalyzed hybridization of H1, H2 remained in the solution (isolated from PDA microtube due to the electrostatic repulsion), suppressing the background leakage signal. Moreover the introduction of mismatched base pairs in H2 could also decrease signal-background ratio significantly. Secondly hydrophilic PDA microtube was placed on OTS-modified hydrophobic substrate. The analyte droplet can be concentrated to a small area after solvent evaporation due to the small interface between the hydrophobic substrate and the droplet. Based on the condensing-enrichment effect, the analyte was enriched and anchored onto the PDA microtube, enhancing the sensitivity.² Particularly, to reduce the uncatalyzed strand exchange, a block which could inhibit nonspecific strand exchange reaction was really important. Thus we introduced mismatched base pairs in H2 which could impede uncatalyzed strand exchange reactions and led to a significant decrease of the signal-background ratio.

Amplification probes (H1, H2) and competitive probes (H') were dissolved into the Tris-acetate/EDTA/Mg²⁺ buffer and separately heated at 95 °C for 10min, followed by slowly annealing to room temperature to ensure the formation of hairpin structure. Single BHQ3@PDA composite microtubes was placed on the OTS coated hydrophobic substrate. Then 20 μ L buffer solution (containing 80 nM H1, 80 nM H2, 10 nM H', the correct target and the mutant target at various concentration) were dropped onto the surface of BHQ3@PDA composite microtubes. For example, the analyst solution contained 80 nM H1a, 80 nM H2a, 10 nM Hc' when we tried to distinguish let-7a and let-7c, regarding let-7a as correct target and let-7c as mutant target. The other experiments were similar to the discrimination between let-7a and let-7c. The droplet would be pinned to the microtube in a small contact area due to the wettability difference between the hydrophilic microtube and its surrounding hydrophobic substrate. After incubating at 25°C for 2 h and rinsing with buffer for several times, the waveguide performance of the composite microtube was characterized by single-tube PL imaging method. The control experiments merely with heterogeneous CHA amplification were carried out without H' at the same conditions. Each test was repeated at least 5 times. The half length of error bar is equal to the value of standard deviation at each condition, and 95% of the data points will be within the region of mean \pm standard deviation.⁵

Stability and reproducibility

First the prepared BHQ3@PDA microtube was heated at 90°C for 5 minutes and rinsed with buffer immediately. Thus the hydrogen bond in probe1-probe2 duplex was broken and the revival of PL intensity could be observed due to the removal of BHQ3 from the surface of PDA microtube (Fig. S6a). Then we used the heated microtube to hybridize with Probe-2 (modified with BHQ3) and found the PL intensity was as low as heated before, indicating the successful anchoring of BHQ3 on the microtube. Two more reproduction and reuse cycles exhibited similar PL intensity variation, clearly verifying that the proposed BHQ3@PDA microtube could serve as a reusable detection

platform. Besides three groups of BHQ3@PDA microtubes were stored at 4 °C with different storage times (0, 5 and 10 days) and employed in discrimination experiments (Fig. S6b).

Temperature and formamide

We have implemented the experiments to study the influence of increasing temperature or adding formamide on the SNV discrimination (Fig. S4). As shown in Fig. S4, upon increasing temperature or addition of formamide, the DF value was found to be varied slightly. Increasing temperature or adding formamide to buffer might speed up DNA hybridization,⁶ however, the hybridization rate of amplification probe with target, or SNV would both be accelerated, only slightly variation in DF values could be obtained in this case.

Discrimination of Let-7 family in clinical samples

The serum samples were extracted from cancer patients and healthy people without further separation and enrichment process. 10 μ L human serum was mixed with 10 μ L buffer solution (containing 160 nM H1, 160 nM H2, 20 nM H') to prepare the analyst solution. Then the above analyst solution was dropped onto the surface of BHQ3@PDA composite microtubes. After incubating at 25°C for 2 h and rinsing for several times, the waveguide performance of the composite microtube was characterized by single-tube PL imaging method. Particularly, the serum samples were treated with the analyst solution containing four amplification probes and one specific competitive probe. For example, pancreatic cancer serum samples were analyzed in four different conditions, containing Ha' or Hc' or He' or Hf', respectively. To prove practicality of this method, a series of discrimination experiments (3-5 serum samples from pancreatic, lung, ovarian, gastric cancer patients and healthy people, respectively) were carried out to distinguish the average expression of let-7a, let-7c, let-7e and let-7f in clinical serum. In heterogeneous CHA amplification strategy, single-stranded (ss-) target miRNA can be enriched onto the surface of PDA microtube due to strong attraction⁴, avoid possible structural damage from enzyme in serum.⁷ Second, the double-stranded (ds-) DNA duplex generated by target catalysis (such as H1-H2) is more stable than ss-miRNA and harder to be degraded.⁸ Therefore the target and CHA components remain intact and active in serum. Therefore, PDA microtube waveguide platform with amplification-competition strategy could be directly applied in 50% serum and the detection can perform really well in real samples.

Table S1 miRNA used in this work.

Name	Sequence
Probe-1 (52)	5'-NH ₂ -CTATAGGCGAACGATT_AACCTAC-3'
Probe-2 (5*)	5'-AATCGTTCGCCTATAG-BHQ3-3'
let-7a (3*2*1*)	5'-TGAGGTA_GTAGGTT_GTATAGTT-3'
let-7c (3*2*1*)	5'-TGAGGTA_GTAGGTT_GTATGGTT-3'
let-7e (3*2*1*)	5'-TGAGGTA_GGAGGTT_GTATAGTT-3'
let-7f (3*2*1*)	5'-TGAGGTA_GTAGATT_GTATAGTT-3'
H1a (12343*2*5*)	5'- AACTATAC_AACCTAC_TACCTCA_TTCAGAGTCC_TGAGGTA_GTAG GTT_AATCGTTCGCCTATAG-3'
H1c (12343*2*5*)	5'- AACCATAC_AACCTAC_TACCTCA_TTCAGAGTCC_TGAGGTA_GTAG GTT_AATCGTTCGCCTATAG-3'

H1e (12343*2*5*)	5'- AACTATAC_AACCTCC_TACCTCA_TTCAGAGTCC_TGAGGTA_GGAG GTT_AATCGTTC GCCTATAG-3'
H1f (12343*2*5*)	5'- AACTATAC_AATCTAC_TACCTCA_TTCAGAGTCC_TGAGGTA_GTAG ATT_AATCGTTCGCCTATAG-3'
Ha' (12343*2*)	5'- AACTATAC_AACCTAC_TACCTCA_CCCAGATGTGTAGA_TGAGGTA_ GTAGGTT-3'
Hc' (12343*2*)	5'- AACCATAC_AACCTAC_TACCTCA_CCCAGATGTGTAGA_TGAGGTA_ GTAGGTT-3'
He' (12343*2*)	5'- AACTATAC_AACCTCC_TACCTCA_CCCAGATGTGTAGA_TGAGGTA_ GGAGGTT-3'
Hf' (12343*2*)	5'- AACTATAC_AATCTAC_TACCTCA_CCCAGATGTGTAGA_TGAGGTA_ GTAGATT-3'
H2a (34*3*2*4)	5'-TACCTCA_GGACTCTGAA_TGAGGTA_GTAGGTA_TTCAGAGTCC- 3'
H2c (34*3*2*4)	5'-TACCTCA_GGACTCTGAA_TGAGGTA_GTAGGTA_TTCAGAGTCC- 3'
H2e (34*3*2*4)	5'-TACCTCA_GGACTCTGAA_TGAGGTA_GGAGGTA_TTCAGAGTCC- 3'
H2f (34*3*2*4)	5'-TACCTCA_GGACTCTGAA_TGAGGTA_GTAGATA_TTCAGAGTCC- 3'
H1(8 nt)	5'- AACTATAC_AACCTAC_TACCTCA_TTCAGAGTCC_TGAGGTA_GTAG GTT_AATCGTTCGCCTATAG-3'
H1(7 nt)	5'- AACTATA_CAACCTAC_TACCTCA_TTCAGAGTCC_TGAGGTA_GTAG GTTG_AATCGTTCGCCTATAG-3'
H1(6 nt)	5'- AACTAT_ACAACCTAC_TACCTCA_TTCAGAGTCC_TGAGGTA_GTAG GTTGT_AATCGTTCGCCTATAG-3'
H1(5 nt)	5'- AACTA_TACAACCTAC_TACCTCA_TTCAGAGTCC_TGAGGTA_GTAG GTTGTA_AATCGTTCGCCTATAG-3'
H1(4 nt)	5'- AACT_ATACAACCTAC_TACCTCA_TTCAGAGTCC_TGAGGTA_GTAG GTTGTAT_AATCGTTCGCCTATAG-3'
H2(D2*M1)	5'-TACCTCA_GGACTCTGAA_TGAGGTA_GTAGGTA_TTCAGAGTCC- 3'
H2(D2*M2)	5'-TACCTCA_GGACTCTGAA_TGAGGTA_GTAGGAA_TTCAGAGTCC-

	3'
H2(D3*M1)	5'-TACCTCA_GGACTCTGAA_CGAGGTA_GTAGGTT_TTCAGAGTCC-3'
H2(D3*M2)	5'-TACCTCA_GGACTCTGAA_CAAGGTA_GTAGGTT_TTCAGAGTCC-3'

Table S2 Comparison of different methods for detection of let-7.

Detection method	Linear range	LOD	Reference
Fluorescence	10-200pM	4.6pM	9
Fluorescence	0.1-100nM	100fM	10
Fluorescence	0-6.25nM	0.81nM	11
SERS	10aM-100fM	6aM	12
SPR	1pM-100nM	270fM	13
Electrochemical	100fM-1nM	99.2fM	14
Magnetic beads	0-100nM	5pM	15

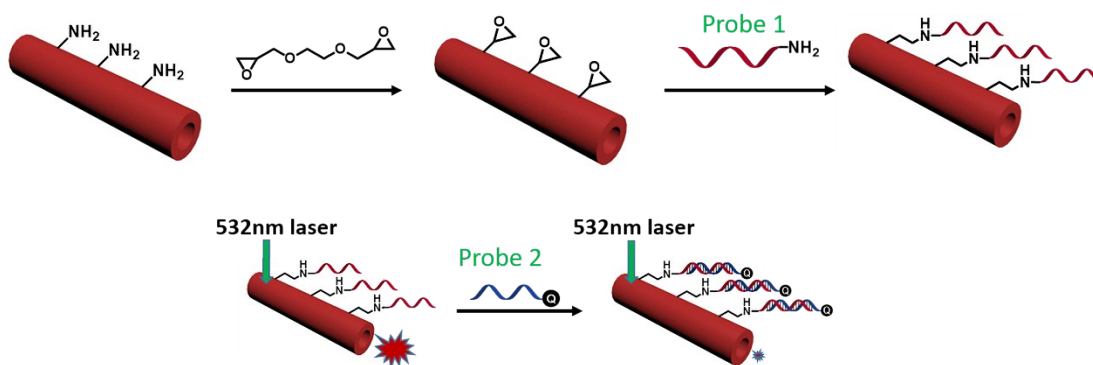


Fig. S1 Preparation of BHQ3@PDA composite microtubes.

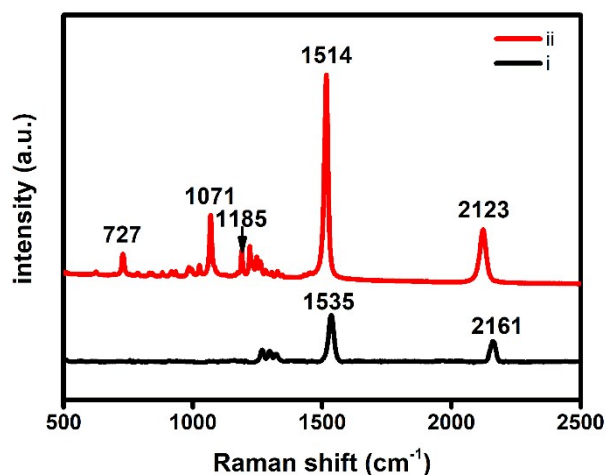


Fig. S2 Raman spectra of (i) epoxy-functionalized PDA microtube and (ii) BHQ3@PDA microtube.

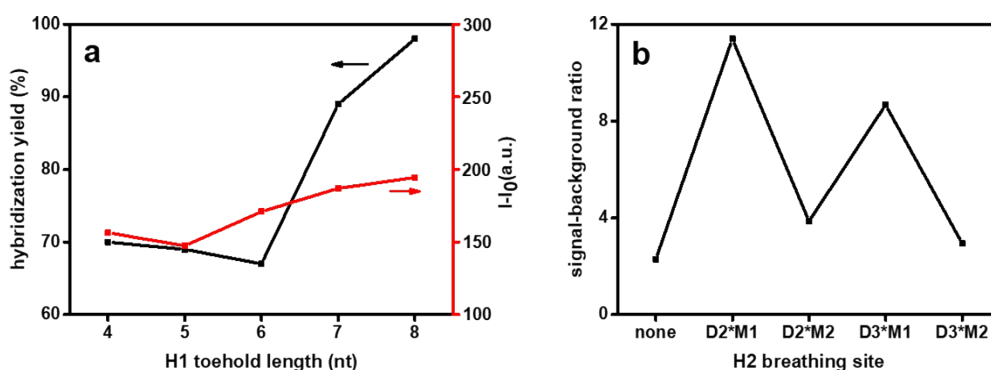


Fig. S3 (a) The hybridization yield between H1 and let-7 (black line) calculated by NUPACK software. The fluorescence enhancement in tip emission of PDA microtube at 640 nm after the addition of different H1 (red line). (b) signal-background ratio with four different mismatches in H2. None: no mismatch in H2; D2*M1: one mismatch in domain 2*; D2*M2: two mismatches in domain 2*; D3*M1: one mismatch in domain 3*; D3*M2: two mismatches in domain 3*. The concentration of H1, H2 and let-7a were 80 nM, 80 nM and 10 pM.

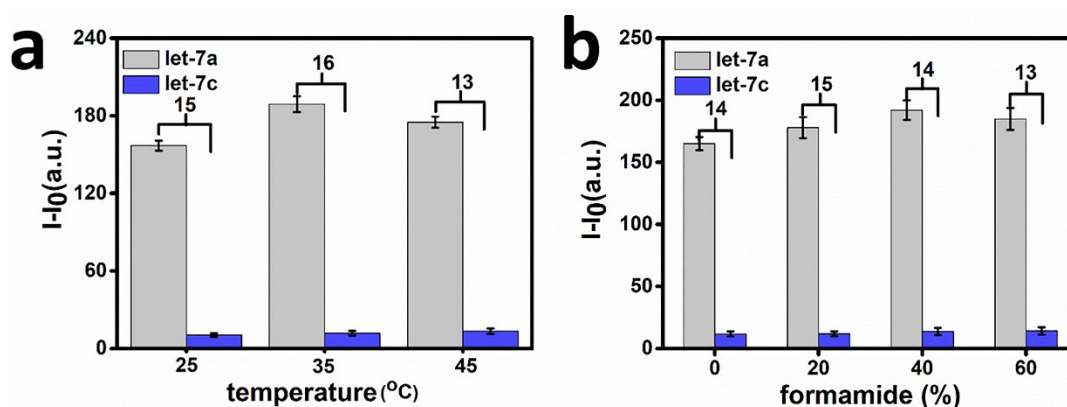


Fig. S4 The tip PL enhancement upon addition of let-7a (gray) or let-7c (blue), (a) at different temperatures, (b) in the buffer containing different volume concentration of formamide. The concentration of let-7a or let-7c was 10pM. H1a, H2a, Hc' were 80nM, 80nM and 10nM respectively in all cases.

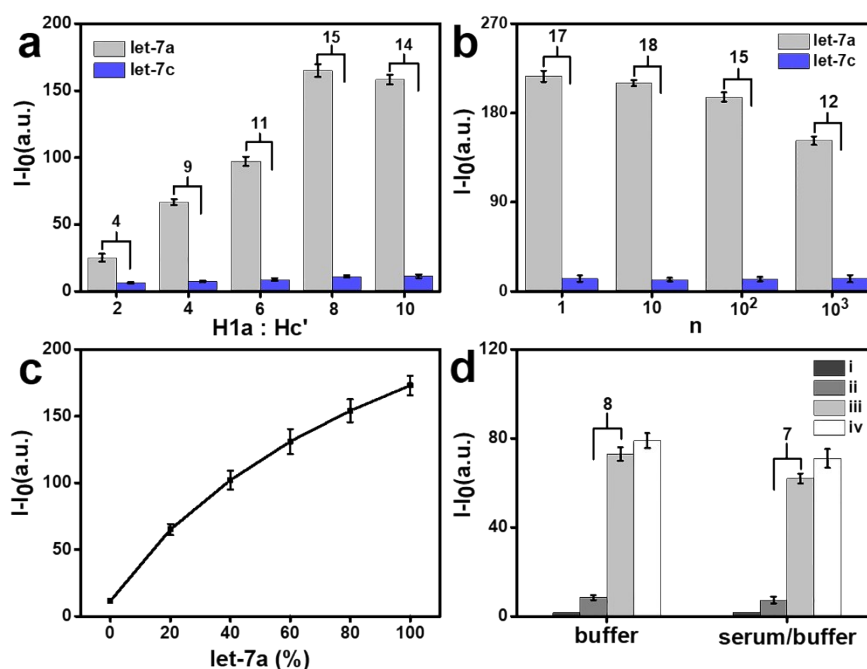


Fig. S5 The tip PL enhancement of PDA microtube at 640 nm after the addition of let-7a or let-7c (a) at various concentration ratios of amplification probe to competitive probe (H1a: Hc'), (b) at various concentration ratios of amplification probe (H1a) to let-7a or let-7c ($n = \frac{[probe]}{[let-7]}$). (c) The fluorescence enhancement in tip emission of PDA microtube at 640 nm upon addition of different let-7a abundances, the total concentration of let-7a and let-7c was 10pM. (d) The fluorescence variation of tip emission for PDA microtube after reaction in different solution (pure buffer or serum/buffer (1: 1, v: v)). (i) blank, (ii) let-7c, let-7e and let-7f, (iii) let-7a, (iv) let-7a, let-7c, let-7e and let-7f. The concentration of let-7a, let-7c, let-7e, let-7f in each analyst solution was the same (0.1pM). The concentration of H1, H2, H' were 80nM, 80nM and 10nM respectively in all cases.

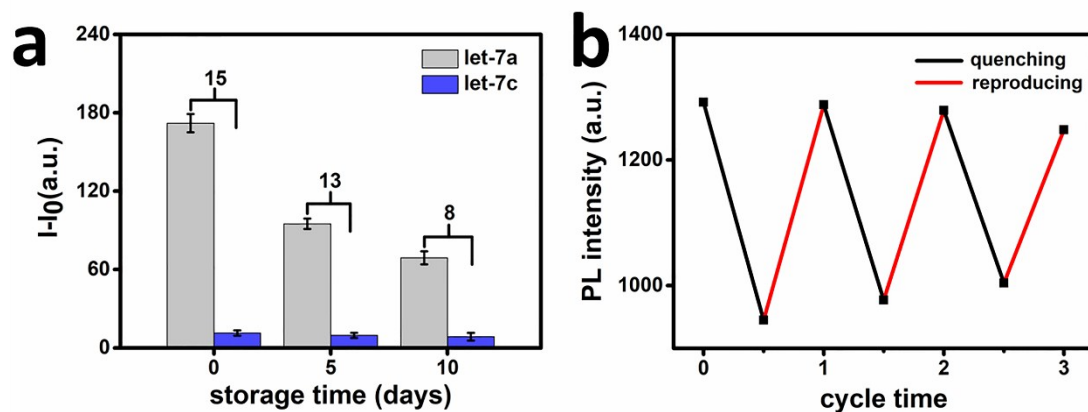


Fig. S6 (a) The tip PL enhancement upon addition of let-7a (gray) or let-7c (blue) at different storage times. (b) The tip PL intensity after quenching and reproducing process. The concentration of let-7a or let-7c was 10pM. H1a, H2a, Hc' were 80nM, 80nM and 10nM respectively in all cases.

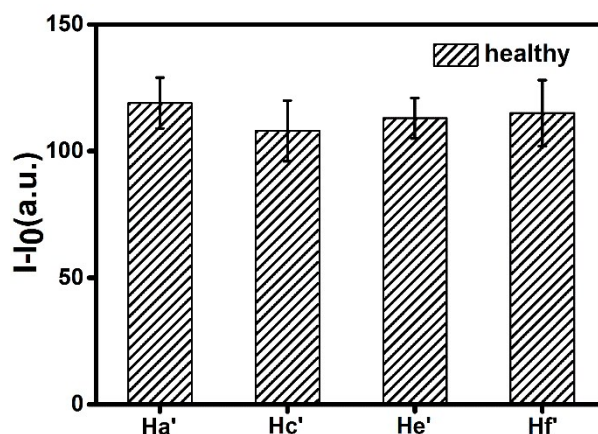


Fig. S7 The tip PL enhancement of PDA microtube at 640 nm after the addition of healthy people serum samples. Each analyst solution contained four amplification probes and one competitive probe (Ha', Hc', He' or Hf'). The concentration of H1, H2, H' were 80 nM, 80 nM and 10 nM respectively in all cases.

The theoretical discrimination factor

The working principle of amplification-competition system based on BHQ3@PDA microtube platform is similar to that of the fluorescent dsDNA probe detection system. Therefore we utilize the method as reported¹⁶ to calculate the theoretical DF. The equilibrium hybridization reaction is:

A+B \rightleftharpoons D+E, where A is the target, B is the probe, D is fluorescent product and E is the duck product.

We define n as the initial concentration ratio between B and A ($n=\frac{[B]_0}{[A]_0}$), χ as the hybridization yield ($\chi=\frac{[D]}{[A]_0}$).

The equilibrium constant:

$$K_{eq}=\frac{[D][E]}{[A][B]}=\frac{[D]^2}{[A][B]}=\frac{\chi^2}{(1-\chi)(n-\chi)} \quad (1)$$

$$\chi_{\infty}=\frac{K_{eq}+K_{eq}\cdot n-\sqrt{K_{eq}\cdot\sqrt{K_{eq}(n-1)^2+4n}}}{2(K_{eq}-1)} \quad (2)$$

When $\Delta G_{target}^{\circ}=-RT\ln K_{eq}=0$, $K_{eq}=1$, $\chi_{target}=\frac{n}{n+1}$.

According to previous research, the value of $\Delta G_{SNV}^{\circ}\approx+6$ kcal/mol at room temperature. There is $K_{eq}=\frac{-\Delta G}{RT}=e^{-10.13}$, the χ_{SNV} could be calculated with different value of n.

Table S3 The hybridization yield of target and SNV and their corresponding DFs at different n.

n	χ_{target}	χ_{SNV}	$\frac{\chi_{target}}{DF}=\chi_{SNV}$
1	0.5	0.0063	79
10	0.909	0.0199	45
100	0.990	0.0615	16
1000	0.999	0.182	5

1. W. Hu, Y. Chen, H. Jiang, J. Li, G. Zou, Q. Zhang, D. Zhang, P. Wang and H. Ming, *Adv Mater*, 2014, **26**, 3136-3141.
2. Y. Zhu, D. Qiu, G. Yang, M. Wang, Q. Zhang, P. Wang, H. Ming, D. Zhang, Y. Yu, G. Zou, R. Badugu and J. R. Lakowicz, *Biosens Bioelectron*, 2016, **85**, 198-204.
3. J. Lee, H. Jun and J. Kim, *Advanced Materials*, 2009, **21**, 3674-3677.
4. C. He, M. Wang, X. Sun, Y. Zhu, X. Zhou, S. Xiao, Q. Zhang, F. Liu, Y. Yu, H. Liang and G. Zou, *Biosens Bioelectron*, 2019, **129**, 50-57.
5. G. Cumming, F. Fidler and D. L. Vaux, *J Cell Biol*, 2007, **177**, 7-11.
6. Z. Zhu, Y. Tang, Y. S. Jiang, S. Bhadra, Y. Du, A. D. Ellington and B. Li, *Sci Rep*, 2016, **6**, 36605.
7. Y. Sun and T. Li, *Anal Chem*, 2018, **90**, 11614-11621.
8. M. Rosa, R. Dias, M. da Graça Miguel and B. Lindman, *Biomacromolecules*, 2005, **6**, 2164-2171.
9. Y. Zhou, J. Zhang, L. Zhao, Y. Li, H. Chen, S. Li and Y. Cheng, *ACS Appl Mater Interfaces*, 2016, **8**, 1520-1526.
10. B. C. Yin, Y. Q. Liu and B. C. Ye, *J Am Chem Soc*, 2012, **134**, 5064-5067.
11. J. Lee, G. Park and D. H. Min, *Chem Commun (Camb)*, 2015, **51**, 14597-14600.
12. M. Zhu, Z. Sun, Z. Zhang and S. Zhang, *Chem Commun (Camb)*, 2018, **54**, 13431-13434.

13. S. Qian, M. Lin, W. Ji, H. Yuan, Y. Zhang, Z. Jing, J. Zhao, J. F. Masson and W. Peng, *ACS Sens*, 2018, **3**, 929-935.
14. Y. Peng, J. Jiang and R. Yu, *Anal. Methods*, 2014, **6**, 2889-2893.
15. X. Wu, B. Guo, Y. Sheng, Y. Zhang, J. Wang, S. Peng, L. Liu and H. C. Wu, *Chem Commun (Camb)*, 2018, **54**, 7673-7676.
16. S. X. Chen, D. Y. Zhang and G. Seelig, *Nat Chem*, 2013, **5**, 782-789.